[American Journal of Science, Vol. 319, September, 2019, P. 529–548, DOI 10.2475/07.2019.01]

American Journal of Science

SEPTEMBER 2019

THE PEDOGENIC FORMATION OF COAL BALLS BY CO_2 DEGASSING THROUGH THE ROOTLETS OF ARBORESCENT LYCOPSIDS

DANIEL O. BREECKER*,† and DANA L. ROYER**

ABSTRACT. Coal balls are calcium carbonate accumulations that permineralized peat in paleotropical Permo-Carboniferous (~320–250 Ma) mires. The formation of coal balls has been debated for over a century yet a widely applicable model is lacking. Two observations have been particularly challenging to explain: 1) the narrow temporal occurrence of coal balls and 2) their typical elemental (high Mg) and isotopic (low $\delta^{18}O$) composition that paradoxically indicate marine and freshwater origins, respectively. We evaluate a new model in which coal balls formed as CO_2 escaped from the peat by diffusion through unusual air-filled spaces in the rootlets of lycopsid trees; critically, these trees were very common in paleotropical mires, and their evolutionary range matches the temporal range of coal balls. The episodic delivery of seawater and marine carbonate sediment to coastal mires is the first step in our model, although other pathways for the delivery of divalent cations are permissible. Subsequent dilution by freshwater and dissolution of these carbonates at the elevated CO_2 of the mire subsurface is followed by the transport of CO_2 through the rootlet airspaces and into the overlying water and atmosphere, which drives carbonate mineral precipitation in the sediment. We show that dilution by freshwater, because it minimally affects Mg/Ca ratios, can result in relatively low pore water $\delta^{18}O$ values while allowing high-Mg calcite formation. This model thus explains the restriction of coal balls to the Permo-Carboniferous and resolves the discrepancy between elemental and isotopic compositions of coal ball carbonate minerals. Furthermore, we show with a 3D reactive transport model that CO_2 could escape rapidly enough through the rootlets to fill 25 percent of the peat pore spaces with calcite before substantial burial (top decimeter of peat), explaining the exceptional preservation of coal swamp flora. Therefore, we suggest that coal balls are pedogenic in origin and that the disappearance of these pedogenically permineralized Histosols represents the first documented decrease in soil diversity on a vegetated planet. The rock record may thus provide important context for the modern loss and degradation of soils.

Keywords: coal balls, arborescent lycopsids, Permo-Carboniferous, soil, diversity

INTRODUCTION

Nodular calcium carbonate accumulations, known as coal balls, permineralize certain Carboniferous and Permian coals, but are notably absent in coals of other ages. Originally described more than a century ago (Hooker and Binney, 1855), coal balls occur in coals across paleotropical Pangea (Phillips, 1980; Tian and others, 1996) and are among the most important paleobotanical archives of the Paleozoic (Taylor and others, 2009). Their often exceptional preservation of plant morphology suggest coal balls usually formed early in the peatification process, perhaps contemporaneous with living plants (Scott and Rex, 1985). Coal ball carbonate minerals can contain trigonal

* Department of Geological Sciences, The University of Texas at Austin, Austin, Texas, 78712.
** Department of Earth and Environmental Sciences, Wesleyan University, Middletown, Connecticut, 06459.
† Corresponding author: breecker@jsg.utexas.edu

prism fibers which suggest formation driven by rapid degassing of CO_2 (Siewers and Phillips, 2015) according to the overall chemical reaction:

$$Ca^{2+} + 2HCO_3^- \rightarrow CaCO_3 + H_2O + CO_2$$

Coal balls typically occur stratigraphically below marine or brackish water deposits (Evans and Amos, 1961; Schopf, 1975) in what were rheotrophic (groundwater-fed) mires (DiMichele and Phillips, 1994). Coal ball mineralogy, normally low and high magnesium calcite, ferroan calcite, dolomite and pyrite (Stopes and Watson, 1909; Perkins, 1976; Love and others, 1983; Rao, 1984; Scott and Rex, 1985; Curtis and others, 1986; Raymond and others, 2012), also suggests a marine influence (for example, Stopes and Watson, 1909; Raymond and others, 2012). In contrast, the plants preserved in coal balls likely grew in freshwater (for example, Raymond and others, 2010), consistent with the $\delta^{18}O$ values of coal ball carbonate minerals which are generally lower (−15‰ to −3‰, PDB) than expected for a pure marine signature (Anderson and others, 1980; DeMaris and others, 1983; Scott and others, 1996; Zodrow and others, 1996; DeMaris, 2000). The wide range of stable carbon isotope compositions of coal ball carbonate minerals (from −35‰ to +1‰ PDB) are thought to record carbon sourced from various combinations of terrestrial plant and marine inorganic endmembers (Weber and Keith, 1962; Anderson and others, 1980; Scott and others, 1996; DeMaris, 2000), with the lowest values probably influenced by methane oxidation (Curtis and others, 1986; DeMaris, 2000).

A conceptual model consistent with these observations, especially the restriction of coal balls to the Permo-Carboniferous and the apparently conflicting evidence for marine and freshwater origins, is currently lacking. Here we evaluate the hypothesis that the escape of CO_2 from pore water by diffusion through air spaces that existed inside the stigmarian rootlets of arborescent lycopsids helped to precipitate the carbonate minerals comprising coal balls.

BACKGROUND

Arborescent Lycopsids

Lycophyta (clubmosses), which contains all fossil and living lycopsids, is one of the first vascular plant clades, appearing by the Late Silurian (Taylor and others, 2009). Extant lycopsids are herbaceous, relatively small in stature, and constitute small fractions of the ecosystem biomass (for example, *Isoetes*) compared with the arborescent Paleozoic life forms, which reached heights of 40 m (DiMichele and Phillips, 1985; Taylor and others, 2009) and dominated Carboniferous coal swamps (fig. 1A). Arborescent lycopsids comprise part of the order Isoetales (Hetherington and Dolan, 2017) and inhabited permanently inundated tropical soils (Phillips and DiMichele, 1992). They had a parichnos system, an unusual vasculature consisting of interconnected voids (aerenchyma) extending through the leaves, stems, and roots (Phillips and DiMichele, 1992; Green, 2010, 2014); this same system is also present in *Isoetes*, the closest extant sister group to the arborescent lycopsids (Green, 2010) (fig. 1C). The root systems of arborescent lycopsids consisted of stigmarian main axes from which stigmarian rootlets radiated in all directions (Taylor and others, 2009). The rootlets, which also contained aerenchyma (Stewart, 1947), branched multiple times and created dense root mats in stands of arborescent lycopsids (Hetherington and others, 2016). Some of the rootlets are thought to have extended out of the peat into the overlying water column (fig. 1B) where CO_2 concentrations were likely lower and O_2 concentrations likely higher than in the peat pore spaces (Phillips and DiMichele, 1992). We suggest that these rootlets created pathways along which CO_2 escaped from the peat pore spaces into the overlying water column, resulting in the precipitation of

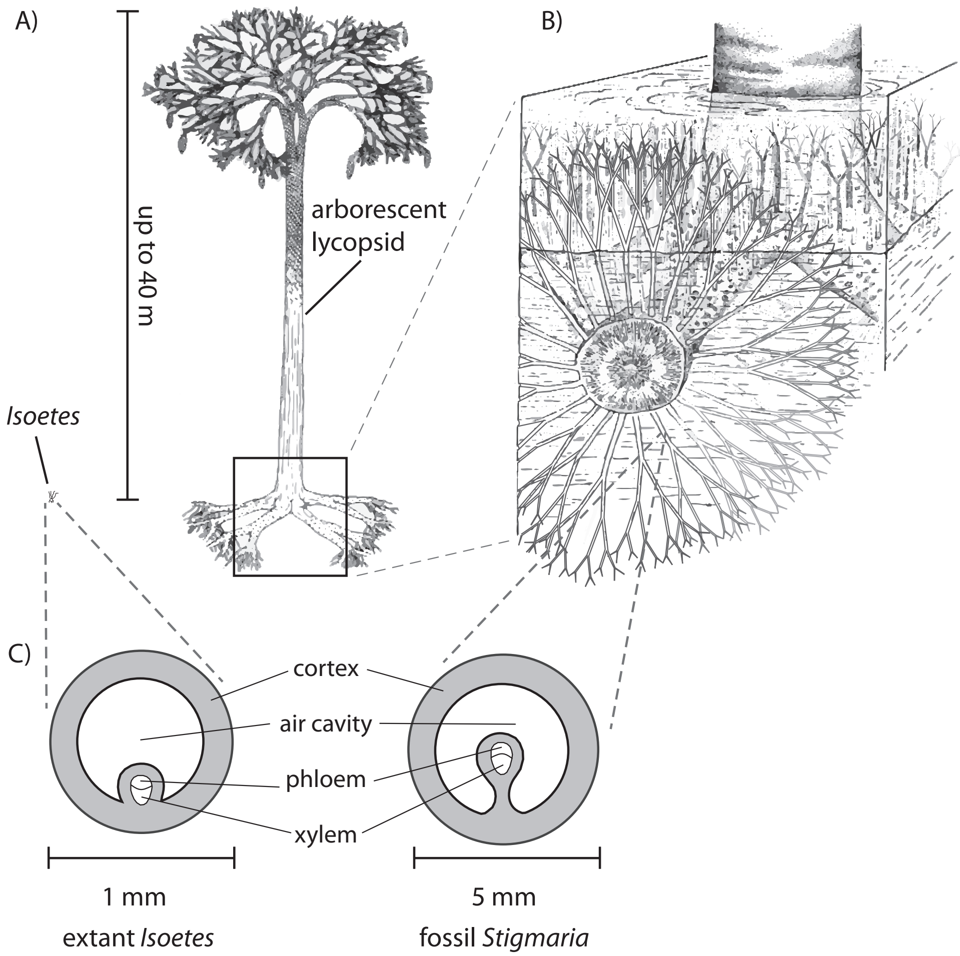

Fig. 1. Morphology and anatomy of arborescent lycopsids. (A) Whole-plant reconstruction (modified from Taylor and others, 2009). Trees were commonly rooted in swamps and could reach 40 m in height. (B) Morphology of root system (*Stigmaria*) (modified from Phillips and DiMichele, 1992). Note that rootlets were present in both the sediment and water column (compare with fig. 4A) and that rootlets branched multiple times forming dense root mats (Hetherington and others, 2016). (C) Cross-section anatomy of rootlets in extant *Isoetes* and fossil *Stigmaria* (modified from Gifford and Foster, 1989). The air cavity is part of the parichnos system.

calcium carbonate in the rhizosphere. The idea that arborescent lycopsids took up—via their parichnos system—large amounts of sedimentary CO_2 for photosynthesis during a ‘bolting’ phase was suggested as a mechanism that helped precipitate coal balls (Green, 2010), but subsequent biophysical calculations cast serious doubt that these plants could bolt (Boyce and DiMichele, 2016). Our modeling does not rely on a bolting phase.

Co-occurrence of Coal Balls and Arborescent Lycopsids

Coal balls are restricted to the paleotropics of the late Paleozoic (dark gray bands in figs. 2B–2D). In Western Europe they range from the late Namurian to Westphalian B/C (~320–315 Ma), in the Donets Basin of Ukraine from Suite G to Suite M (~318–309 Ma), and in North America from the early Atokan to late Virgilian

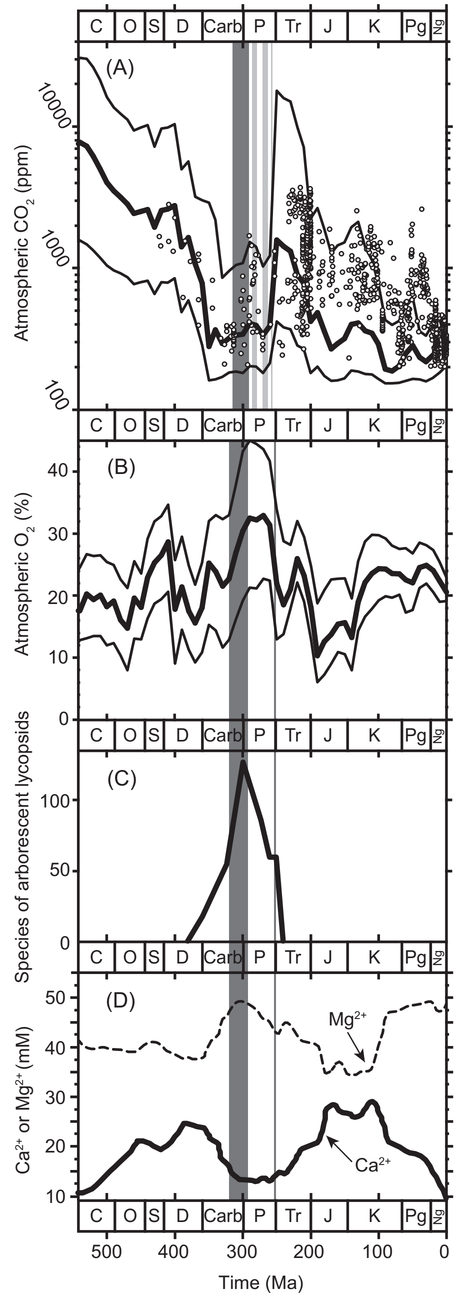

Fig. 2. Phanerozoic patterns in climate, arborescent lycopsid diversity, coal ball occurrence, and seawater chemistry. (A) Atmospheric CO_2. Solid line and 95% confidence interval come from the long-term carbon cycle model GEOCARBSULFvolc (Berner, 2006b; Royer and others, 2014). Circles are individual proxy CO_2 estimates (updated from Royer, 2014). The dark gray band is the interval of peak glaciation during the Permo-Carboniferous; the light gray bands represent glacial times that were more regional in scope (Isbell and others, 2012). (B) Atmospheric O_2. Solid line and 95% confidence interval from the long-term carbon cycle model GEOCARBSULFvolc (Berner, 2009; Royer and others, 2014). (C) Species richness of arborescent lycopsids (Niklas and others, 1985). (D) Simulated Ca and Mg concentrations of Phanerozoic seawater (Farkas and others, 2007). Dark gray bands in panels B-D mark the periods where coal balls are present (see main text). All ages follow the GTS 2012 (Gradstein and others, 2012). Modified from Green (2010).

(~317–299 Ma) (Phillips, 1980; Phillips, 1981; Phillips and others, 1985). In China, the oldest coal balls are late Namurian in age and occur regularly through the Asselian/early Sakmarian (~320–295 Ma); after a 40 m.y. hiatus, they are present again in the Changhsingian at the end of the Permian (~254–252 Ma) (Li and others, 1995; Tian and others, 1996; Hilton and others, 2001; Wang and others, 2003; Spencer and others, 2013).

Coal balls occur during a geologically unprecedented peak in atmospheric O_2 exceeding 25 percent (Green, 2010) (fig. 2B). The stratigraphic range of coal balls also aligns with low atmospheric CO_2 (fig. 2A) and cool, glacial climates in the higher latitudes. The interval of peak glacial activity (dark gray band in fig. 2A) (Isbell and others, 2012) coincides almost exactly with the main phase of coal ball formation. Glacial deposits are not known from the younger coal ball phase in the late Permian, but global temperatures at that time may have been low (Chen and others, 2013).

The species richness of arborescent lycopsids (Niklas and others, 1985) closely tracks coal ball occurrence (Green, 2010) (fig. 2C). Lycopsids commonly comprise >70 percent of identifiable material in coal balls (Phillips and Peppers, 1984; DiMichele and Phillips, 1985; Phillips and others, 1985; Liand others, 1995). In North America, the decline of arborescent lycopsids unambiguously parallels the decline of coal balls (Phillips and Peppers, 1984; Phillips and others, 1985), with the youngest coal balls during the Virgilian containing very little lycopsid material (Phillips, 1980; Phillips and others, 1985). While arborescent lycopsids go extinct in North America and Europe ~303 Ma, they persist in China through the end of the Permian (Li and Yao, 1982; Wang, 1985; Li and others, 1995) and are present in Changhsingian coal balls (Li and others, 1995; Tian and others, 1996). Clearly, coal balls are closely associated with arborescent lycopsids, with a majority of coal balls containing lycopsids as the most substantial botanical material (DiMichele and Phillips, 1985).

Previous Models for Coal Ball Formation

Coal ball formation was originally explained by the presence of marine shells in overlying shales (Hooker and Binney, 1855). Later models suggested that marine transgression of coastal mires followed by sulfate reduction resulted in the precipitation of pyrite and carbonate minerals (Stopes and Watson, 1909; Curtis and others, 1986). The observation of marine fauna at the core of some coal balls led to the idea that marine carbonate mud rollers served as nuclei for coal balls (Mamay and Yochelson, 1962). However, most coal ball carbonate minerals have relatively low $\delta^{18}O$ values, suggesting formation from freshwater (Scott and others, 1996) such as carbonate-rich springs (Anderson and others, 1980). Two other models involve buried peat: 1) burial of peat beneath the freshwater lens of coastal swamps (Spicer, 1989) and 2) erosional unroofing of buried peat resulting in CO_2 degassing and carbonate precipitation (DeMaris and others, 1983; DeMaris, 2000).

None of these models reconcile all observations of coal balls, leading some (Scott and others, 1996) to conclude that no single mechanism explains the formation of all coal balls. Importantly, none of these models explains the restriction of coal balls to the Permo-Carboniferous. Furthermore, none of these models describes a pedogenic mechanism for coal ball formation and thus these deposits have not been widely recognized as soils, although a pedogenic origin has been hypothesized and some of these models are consistent with the formation of coal balls at shallow depths in peat (Stopes and Watson, 1909; Anderson and others, 1980). We describe and test a new model for coal ball formation that incorporates aspects of these previous models and suggests that the permineralization was a pedogenic process.

PEDOGENIC PERMINERALIZATION OF PERMO-CARBONIFEROUS PEATS

A New Model for Coal Ball Formation

The first step in our model for pedogenic permineralization of peat is the episodic delivery of seawater and calcium carbonate-bearing marine sediment to coal swamps (Mamay and Yochelson, 1962; Perkins, 1976). This delivery may have occurred during tropical cyclones (Tweel and Turner, 2012) or smaller scale washover, or perhaps along brackish tidal channels. These carbonate minerals and the seawater itself are the source of divalent cations (Ca^{2+}, Mg^{2+}, Sr^{2+}). Following delivery to coastal swamps, the seawater was variably diluted by freshwater and the carbonate minerals dissolved under the elevated P_{CO2} (from decomposition of organic matter) of the mire subsurface. Finally, as pore waters moved laterally into stands of arborescent lycopsids, some of the CO_2 was transported out of the peat through rootlets, driving calcium carbonate precipitation, consistent with the trigonal prisms of calcite in coal balls that suggest calcite formation was driven by CO_2 degassing.

This conceptual model is consistent with the geochemistry of typical calcium carbonate-dominated coal balls. The evidence for both marine and freshwater origins of coal balls suggests that coal balls formed from mixtures of seawater and freshwater. Such an explanation has been problematic, however, because most seawater-freshwater mixtures are undersaturated with respect to calcite (for example, Dreybrodt, 1981). The escape of CO_2 through lycopsid rootlet airspaces explains how calcite could precipitate from such mixtures.

The challenge of explaining low $\delta^{18}O$ values of high-Mg calcite is illustrated in figure 3A. Mixtures of seawater and freshwater have Mg/Ca ratios equal to that of seawater, but are typically under-saturated with respect to calcite. Dissolution of $CaCO_3$ after seawater-freshwater mixing could result in saturation with respect to calcite, priming the solution for mineralization of peat, but would also decrease the Mg/Ca of the solution. All else being equal, the amount of decrease in Mg/Ca would be larger for mixtures with a larger fraction of freshwater because mixing with freshwater decreases the concentration of Mg in solution, making the Mg/Ca ratio more susceptible to change. To test whether our model can explain the observed low $\delta^{18}O$ values of coal ball high-Mg calcite, we calculated the $\delta^{18}O$ values of calcite in equilibrium with seawater-freshwater mixtures that reached saturation with respect to calcite at elevated P_{CO2} but maintained sufficiently high Mg/Ca to form high-Mg calcite (fig. 3B). Specifically, the conceptual model explains $\delta^{18}O$ values of high-Mg calcite that are less than -5 permil, which are difficult to explain by formation from seawater alone unless formation temperatures exceeded 30 °C (fig. 3B). We emphasize that CO_2 escape from peat through stigmarian rootlets could drive carbonate mineral precipitation from waters with other divalent cations sources, provided Mg/Ca ratios were sufficiently high, and thus a marine divalent cation source is not required.

Coal ball calcites with the highest observed $\delta^{18}O$ values of -3 permil (Scott and others, 1996) are consistent with formation from seawater at 20 °C. Most coal ball calcites have $\delta^{18}O$ values between -8 and -3 permil (Scott and others, 1996), which can be explained by reasonable tropical, coastal Pennsylvanian freshwater endmember $\delta^{18}O$ values of -7 permil (SMOW) or higher (fig. 3). Alternatively, higher calcite formation temperatures and/or lower peat pore water CO_2 (and thus larger freshwater dilutions while maintaining Mg/Ca >2) might help explain high Mg calcite $\delta^{18}O$ values at the low end of this range. Even lower coal ball carbonate mineral $\delta^{18}O$ values (as low as $-15‰$) are likely explained by recrystallization during diagenesis (Scott and others, 1996). The highly negative $\delta^{13}C$ values of some coal ball carbonate minerals can be explained by methane oxidation (Curtis and others, 1986; DeMaris, 2000), perhaps accommodated by belowground O_2 transport to the rhizosphere through the rootlets of arborescent lycopsids.

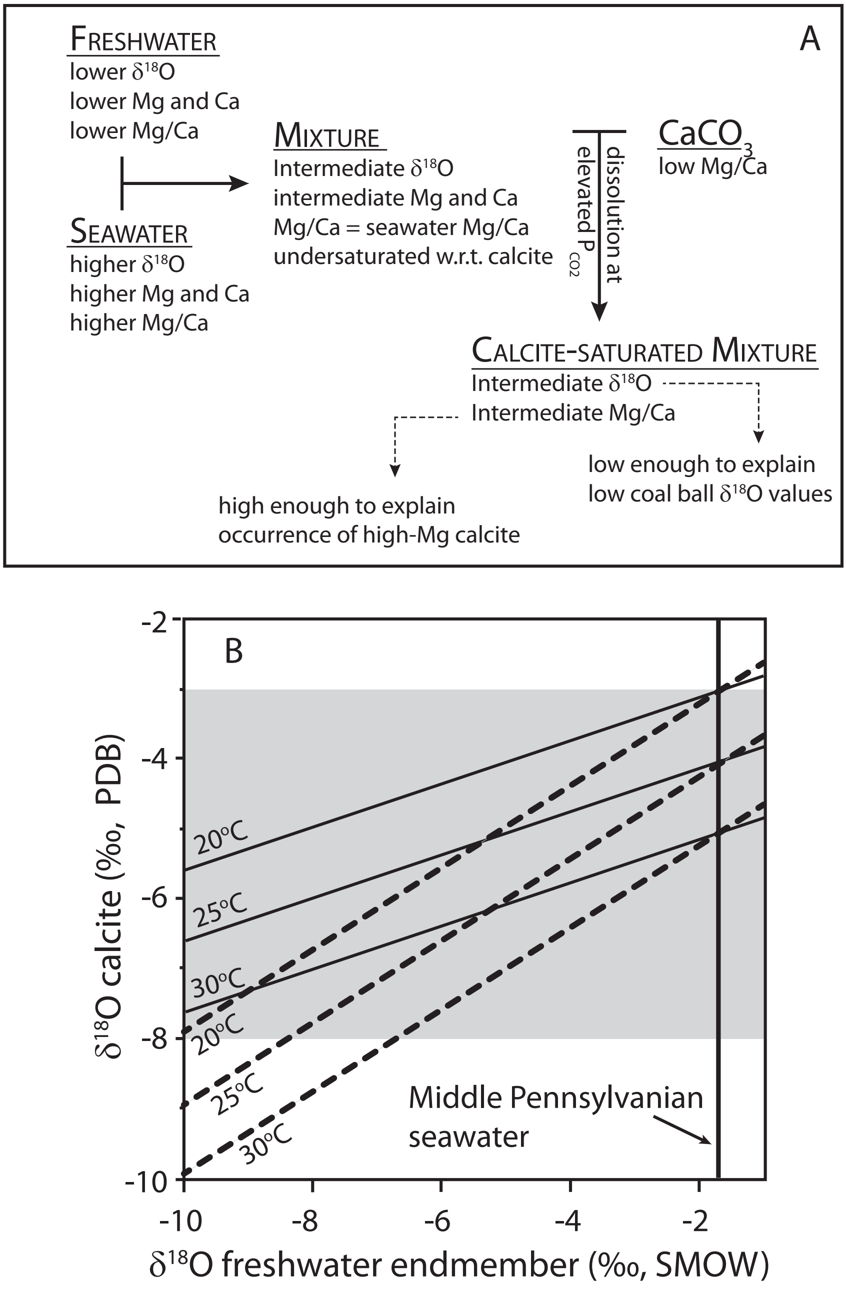

Fig. 3. The formation of high-Mg calcite with low δ^{18}O values. (A) Schematic diagram illustrating the challenges associated with explaining low δ^{18}O values of high-Mg calcite. (B) Oxygen isotope compositions of calcite in equilibrium with mixtures of seawater and freshwater. The fraction of freshwater used here is the fraction that results in pore water Mg/Ca = 2 (lower limit for high Mg calcite) assuming waters equilibrate with calcite at P_{CO2} = 0.1 atm after mixing. This gives the maximum dilution by freshwater, and thus the lowest δ^{18}O values that are consistent with formation of high-Mg calcite. Seawater δ^{18}O value set to −1.7‰ (SMOW) (Came and others, 2007). The solid and dashed diagonal lines are for minimum and maximum, respectively, Mg/Ca ratios of seawater during episodes of coal ball formation (Farkas and others, 2007) as shown in figure 2. The range of most coal ball δ^{18}O values (−8 to −3‰, Scott and others, 1996) is shown in gray.

Coal balls occur 1) below channels eroded into coals and overlying shales (DeMaris and others, 1983), 2) as accumulations with convex upper surfaces (Evans and Amos, 1961), and 3) in 'pockets' with fewer if any coal balls in the surrounding coal (Stopes and Watson, 1909). We suggest that such lateral heterogeneity of coal ball occurrence might be explained by paleoecotones in the coal swamps such that coal balls preferentially formed on disturbed surfaces colonized by opportunistic arborescent lycopsids (DiMichele and DeMaris, 1987; Baker and DiMichele, 1997). Lateral heterogeneity might also be explained by an association of coal balls with brackish tidal channels, which are known to result in spatially heterogeneous marine influences on Holocene coastal mires (Phillips and Bustin, 1996). Also, our model involves laterally flowing waters that lose Ca^{2+} by calcium carbonate precipitation as they moved through the rhizosphere of coal swamp trees. Thus, our model implies that there were limitations to the horizontal distances over which coal balls could form; coals balls would preferentially form where flowing waters first encountered dense roots mats of aerenchymatous coal swamp trees. It is therefore possible that the presence of such 'fronts' of coal balls might have influenced the locations of channels eroded into the superjacent shales, rather than vice versa as suggested previously (DeMaris and others, 1983).

Biogeochemical Plausibility Assessment

Could CO_2 escape from pore waters by diffusion through rootlets drive rapid enough calcite precipitation to lithify the peat and prevent compaction? To address this question, we simulated CO_2 escape from peat and the resulting calcite precipitation using a 3D reactive transport model. The model contained a layer of water overlying a layer of peat. Two closely-spaced branching stigmarian rootlets extended upward through the peat and the distal rootlet tips extended into the overlying water column (fig. 4). The rootlets consisted of an outer cortex and an inner air space. Water flowed laterally into the model and around the rootlets and CO_2 was allowed to exchange by diffusion across the outer cortex between the water or water-filled pore space and the air space inside the rootlet. The lowering of CO_2 in proximity to rootlets in the peat drove calcite precipitation, the steady state rates of which were calculated using COMSOL Multiphysics® (COMSOL Inc.).

Model geometry and water flow.—We considered two identical branching rootlets spaced center-to-center 1 cm apart in the y-direction. The model rootlets were oriented vertically (z-direction). The main stems of each rootlet extended 10 cm directly upward from the origin and branched 4 times all in the same plane (the x-z plane) into successively shorter sections that were 9.2, 8.5, 7.8 and 7.2 cm in length. From proximal to distal, the inner angles between the branches were, 28°, 20°, 16° and 12°, the outer diameters of the rootlet sections were 0.8, 0.584, 0.424, 0.312, 0.224 cm and the outer diameters of the airspaces inside each section of the rootlets were 0.5, 0.365, 0.265, 0.195 and 0.140 cm. This geometry is based on observations of stigmarian systems of fossil arborescent lycopsids (Stewart, 1947; Hetherington and others, 2016). In COMSOL, spheres were used to join the rootlet sections together such that the airspace was continuous throughout the rootlets. We considered the half of these rootlets that were in the region $x < 0$ (that is divided symmetrically through the first branch point).

The rootlets extended through a layer of water-saturated peat and up into a layer of water (representing the overlying water column). The peat layer had dimensions 32 cm tall (z) × 25 cm wide (x) × 1 cm deep (y). The water column on top of the peat had the same width and depth and was 10.6 cm tall, extending just above the distal ends of the rootlets. The $y = 0$ and $y = 1$ cm planes, which bisected the rootlets vertically, were considered symmetry boundaries (mirror symmetry of flow and mass flux and thus no flow or flux across the boundary) in the calculations. The top of the water column was also considered a symmetry boundary for water flow. The bottom of the peat and the

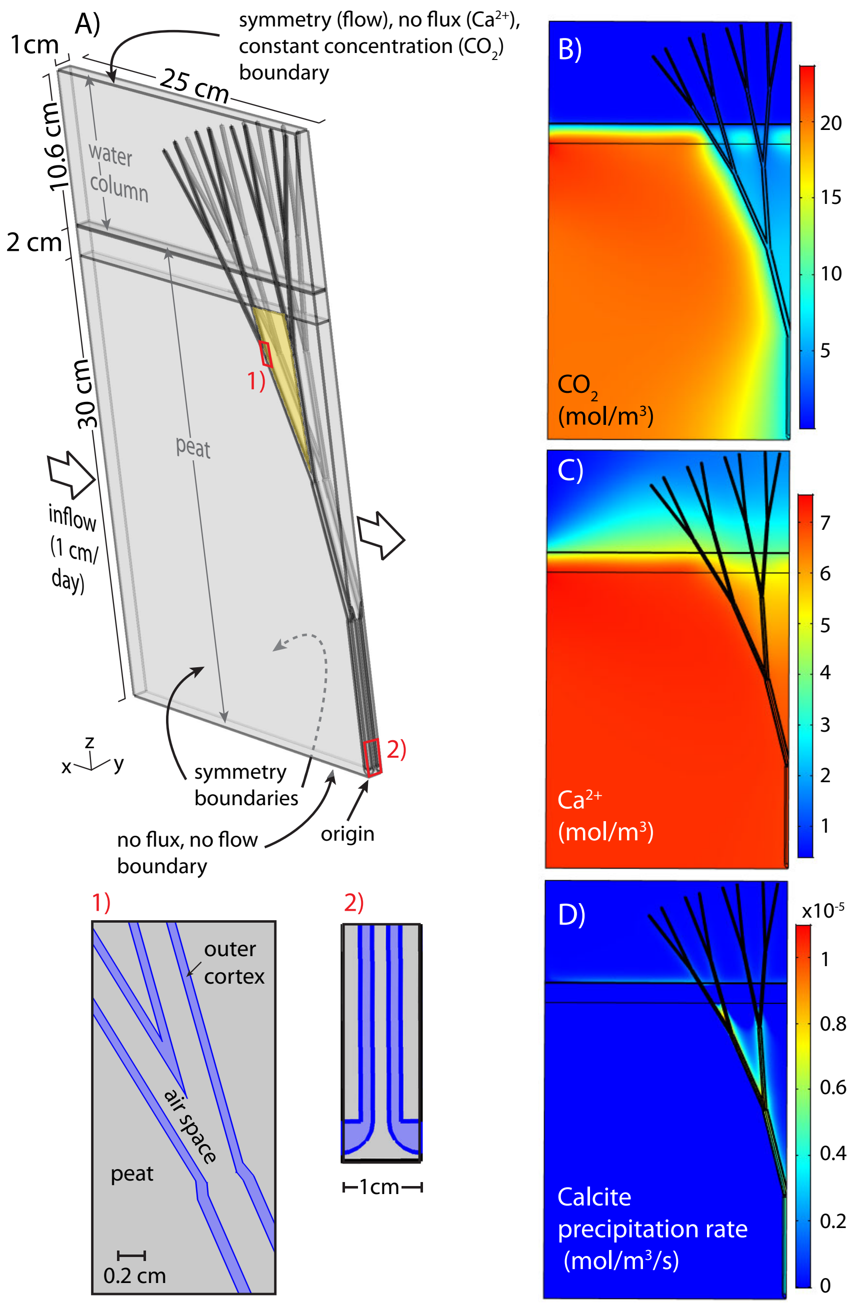

Fig. 4. Model geometry and results. Dimensions and boundary conditions with insets showing detail (A). CO_2 is consumed by photosynthesis in the water column and produced by respiration in the top layer of the peat. Water flows in from the left at a rate of 5 mm/day and flows around the rootlets. Rapid transport through the airspaces leads to low CO_2 in the rhizosphere (B) which results in calcite precipitation and lowering of Ca^{2+} concentrations (C). The calcite precipitation rates (D) within the yellow highlighted region (a) were averaged to estimate the percentage of pore space that could be permineralized with calcite in the soil zone. Calcite dissolution occurs in the top 2 cm of the peat and is not shown here. Concentrations and rates are shown per cubic meter water.

outside of the rootlets were considered no flow boundaries at which water velocity was set to zero. Water flowed in on the left (through the plane x = −25) and out on the right (through the plane x = 0). The distance upstream from the rootlet allowed steady state to be achieved before the flow interacted with the rootlet. Water flow was considered to be laminar, which is reasonable given the relatively low prescribed velocities of 0.2 mm to 5 cm/day (Reynolds, 1883). Water flow in our simulations did not occur in the outer cortex or the airspaces of the rootlet. By doing this, we ignore transpiration, which we consider reasonable given that transpiration must have been much smaller than groundwater flow in the everwet, groundwater-fed swamps in which coal balls formed. Considering transpiration would increase the rate of CO_2 escape because water would be drawn toward the rootlets, moving CO_2 toward the sink faster than by diffusion alone. Therefore, by not considering transpiration we simulate conservatively small calcite precipitation rates. Our model does not involve transport in the parichnos between roots and shoots. Only CO_2 transport within individual rootlets is considered, which is reasonable given the existence of tissue between rootlets and stigmarian main axes which would have acted as substantial barriers to diffusive transport from roots to shoots (Boyce and DiMichele, 2016).

Solutes: carbon and calcium.—CO_2 was produced in the top 2 cm of the peat at a rate of 9.7×10^{-5} mol/m^3/s, which is the mean respiration rate measured in modern tropical and subtropical peat swamp forests (Bridgham and Richardson, 1992; Chimner, 2004; Sundari and others, 2012). CO_2 was consumed in the water column at a rate proportional to the difference between the CO_2 concentration in the water and the aqueous CO_2 concentration in equilibrium with a prescribed atmospheric value of 200 ppmV, which maintains the CO_2 concentration in the water at a level very close to equilibrium with the atmosphere. The model is very insensitive to the atmospheric CO_2 level used because the fluxes calculated are controlled by the difference between peat CO_2 (>0.1 atm) and atmospheric CO_2 (<0.01 atm).

The diffusion coefficients for CO_2 within the model were assigned as follows: 1.92×10^{-9} m^2/s in the water column, representing diffusion in water (Cussler, 2009), 9.6×10^{-10} m^2/s in the peat and the outer cortex of the rootlets, which is smaller than in water due both to the porous nature of peat and to the presence of cellulose in the outer cortex, and 6.5×10^{-7} m^2/s in the air spaces. The latter was calculated using the diffusion coefficient for CO_2 in air (Massman, 1998) and accounting for an estimated 50 percent porosity of the aerenchyma, a conservative estimate based on the work of Stewart (1947), elevated atmospheric pressure (1.15 atm) due to higher atmospheric O_2 concentrations (Berner, 2006a) that characterized the time period of coal ball formation (fig. 2B), and the dimensionless Henry's law constant of 0.83 accounting for the different volumetric concentrations of CO_2 in air and water. The diffusion coefficients for Ca^{2+} were assigned as 1.34×10^{-9} in the water column and 6.72×10^{-10} m^2/s in the peat, a factor of 0.7 times the diffusion coefficients for CO_2 (Buhmann and Dreybrodt, 1985). The bottom of the peat was defined as a no flux boundary for CO_2 and Ca^{2+} and the outside of the rootlets were defined as no flux boundaries for Ca^{2+}(Ca^{2+} was not transported into or through the rootlets in our model). The top of the water column was defined as a constant concentration boundary for CO_2 (0.0068 mol/m^3,the value in equilibrium with a prescribed atmospheric CO_2 concentration of 200 ppmV) and a no flux boundary for Ca^{2+}. The inflow concentrations of CO_2 and Ca^{2+} were set as their steady state values in the absence of rootlets. Diffusion of HCO_3^- was not considered. Gradients in HCO_3^- are much smaller than gradients in CO_2 for the problem being considered. This is because CO_2 diffuses rapidly out of the peat through the airspaces in the rootlets resulting in low CO_2 in the surrounding peat whereas HCO_3^- concentrations are only substantially decreased by calcite precipitation, which is relatively slow compared to CO_2 escape. Thus HCO_3^-

concentrations surrounding the rootlets is not lowered nearly as much as is CO_2. This along with the larger diffusion coefficient for CO_2 than HCO_3^- in solution means that diffusive carbon transport occurs primarily by CO_2 and that ignoring HCO_3^- diffusion is reasonable.

Calcite dissolution/precipitation kinetics.—The rates of calcite dissolution were calculated using the Plummer-Wigley-Parkhurst equation (Plummer and others, 1978):

$$R_{diss} = \kappa_1(A_{H+}) + \kappa_2(A_{H2CO3*}) + \kappa_3 - \kappa_4(A_{Ca2+})(A_{HCO3-}) \tag{1}$$

where $A_{H2CO3*} = A_{H2CO3} + A_{CO2}$, and κ and A denote rate constants and activities, respectively. Equilibrium among dissolved inorganic carbon species was assumed in order to calculate activities for use in equation (1), which is robust when the ratio of the dissolving fluid to the surface area of the calcite is large (Dreybrodt, 1980) and/or when carbonic anhydrase is present (Dreybrodt and others, 1997), as expected for organic carbon-rich waters such as those in peat. We used the originally reported values of κ_1, κ_2 and κ_3 for 25 °C (Table 1 in Plummer and others, 1978). The values of κ_4 were determined using a continuous function, $\kappa_4 = f(CO_2)$, newly determined in this work. To do this, equation (1) was first solved for κ_4 and then values of the other variables at equilibrium with respect to calcite (that is precipitation rate = 0 and equilibrium values of $A_{H+}, A_{Ca2+}, A_{HCO3-}$) were used to calculate κ_4 at various P_{CO2}. A 6^{th} order polynomial was fitted to κ_4 versus $\log_{10}(P_{CO2})$, resulting in the following expression, which closely matches the data reported by Plummer and others (1978):

$$\kappa_4 = 7.947e\text{-}4(x^6) + 6.265e\text{-}3(x^5) + 2.186e\text{-}2(x^4) + 3.454e\text{-}2(x^3) + 3.251e\text{-}2(x^2) + 1.792e\text{-}2(x) + 1.92e\text{-}2 \tag{2}$$

where $x = \log_{10}(P_{CO2})$ and P_{CO2} has units of atmospheres and the calculated value of κ_4 has units $cm^4\ mmol^{-1}\ s^{-1}$. Rates calculated using equation (1) are relative to calcite surface area. To calculate a volumetric rate, we used calcite surface areas of 1×10^{-4} m^2/L in the water column ($s_{watercolumn}$) and 1×10^{-2} m^2/L in the peat (s_{peat}), the latter of which represents trace amounts of calcite (<0.01 wt %) assuming the surface area of foraminifera (de Kanel and Morse, 1979).

Calcite precipitation rates were calculated using equations that consider the sorption of dissolved organic carbon (DOC) on calcite crystal surfaces (Lebron and Suarez, 1998):

$$R_{CG} = s(k_{CG})(A_{Ca^{2+}}A_{CO_3^{2-}} - K_{SP})\psi_{CG}P_{CO_2}(DOC)^{\theta_{CG} + \lambda_{CG}\log_{10}(P_{CO_2}+1)} \tag{3}$$

$$R_{HN} = k_{HN} * f(SA)(\log_{10}(\Omega - 1.5))\psi_{HN}P_{CO_2}(DOC)^{\theta_{HN} + \lambda_{HN}\log_{10}(P_{CO_2}+1)} \tag{4}$$

$$R_T = R_{CG} + R_{HN} \tag{5}$$

where the *R's* are rates of calcite precipitation ($mol/m^3/s$) and the subscripts *CG*, *HN* and *T* refer to crystal growth, heterogeneous nucleation and total calcite precipitation, respectively. In these equations, s is calcite surface area (m^2/L) and SA is particulate surface area that facilitates heterogeneous nucleation; f(SA) = 1 when particulate surface area is 0, the condition assumed in this work. The *k's* are the precipitation rate constants, K_{SP} is the solubility product for calcite, Ω is the calcite saturation state defined by $A_{Ca^{2+}}A_{CO_3^{2-}}/K_{SP}$. Values of activity coefficients were approximated from $[Ca^{2+}]$ using curves relating activity coefficients to $[Ca^{2+}]$ at equilibrium with calcite. *DOC* is the concentration of dissolved organic carbon (mmol/L), P_{CO2} is CO_2 pressure in kPa, and ion activities have units of mmol/L. The variables ψ, θ and λ are experimentally determined constants (Table 1 in Lebron and Suarez, 1998).

TABLE 1

Values of input variables

variable	description	value	units	references/notes
$D_{CO2\text{-}outercortex}$	CO_2 diffusion coefficient in outer cortex of rootlets	$9.6*10^{-10}$	m^2/s	half the value of pure water, largest unknown in modeling
V_{water}	inflow velocity of water	5	mm/day	Gafni and Brooks, 1990
DOC	dissolved organic carbon concentration in peat pore water	5	mM	Gandois and others, 2013; Moore and others, 2013; Müller and others, 2015
R	respiration rate in peat (top 2 cm)	$9.7*10^{-5}$	$mol/m^3/s$	Bridgham and Richardson, 1992; Chimner, 2004; Sundari and others, 2012
s_{peat}	calcite surface area in peat	$1*10^{-2}$	m^2/L	assumed, results not sensitive to this value
SA	other particulate surface area	0		conservative assumption
AR	peat accumulation rate	2	mm/yr	Dommain and others, 2011; Falcon-Lang, 2004; Nadon, 1998
$s_{watercolumn}$	calcite surface area in water column	$1*10^{-4}$	m^2/L	assumed, results not sensitive to this value
$D_{CO2\text{-}peat}$	CO_2 diffusion coefficient in peat	$9.6*10^{-10}$	m^2/s	Cussler 2009
$D_{CO2\text{-}watercolumn}$	CO_2 diffusion coefficient in water column	$1.92*10^{-9}$	m^2/s	Cussler 2009
$D_{CO2\text{-}rootlet\ airspaces}$	CO_2 diffusion coefficient in rootlet air spaces	$6.5*10^{-7}$	m^2/s	assumes porosity of 0.5 (conservative based on Stewart 1947) and atm pressure 1.15x modern (Berner 2006a)
$D_{Ca2+\text{ - }peat}$	Ca^{2+} diffusion coefficient in peat	$6.72*10^{-10}$	m^2/s	Buhmann and Dreybrodt, 1985
$D_{Ca2+\text{ - }watercolumn}$	Ca^{2+} diffusion coefficient in water column	$1.34*10^{-9}$	m^2/s	Buhmann and Dreybrodt, 1985
κ_1	rate constant in equation (1)	$5.11466*10^{-4}$	m/s	Plummer and others, 1978
κ_2	rate constant in equation (1)	$3.45387*10^{-7}$	m/s	Plummer and others, 1978
κ_3	rate constant in equation (1)	$1.19337*10^{-6}$	$mol/m^2/s$	Plummer and others, 1978
k_{CG}	rate constant for calcite crystal growth	64.8	$L^2/mmol/m^2/s$	Lebron and Suarez 1998
k_{HN}	rate constant for heterogeneous nucleation of calcite	$7.82*10^{-4}$	$mmol/m^2/s$	Lebron and Suarez 1998
ψ_{CG}	fitted constant [1]	$8.57*10^{-6}$		Lebron and Suarez 1998
θ_{CG}	fitted constant [1]	-3.052		Lebron and Suarez 1998
λ_{CG}	fitted constant [1]	0.793		Lebron and Suarez 1998
ψ_{HN}	fitted constant [1]	$5.916*10^{-3}$		Lebron and Suarez 1998
θ_{HN}	fitted constant [1]	-1.41		Lebron and Suarez 1998
λ_{HN}	fitted constant [1]	0.61		Lebron and Suarez 1998
ϕ	initial peat porosity	0.5		conservative assumption
T	temperature	25	°C	assumed

[1] constant in rate expression for calcite nucleation

The rate limitation imposed by CO_2 production at the site of calcite precipitation (Dreybrodt, 1980) was explicitly considered by including the precipitation/dissolution rate as a CO_2 source/sink term (that is added to the respiratory/photosynthetic fluxes to determine the total CO_2 produced or consumed at each node). For $\Omega < 1$, equation (1) was used to calculate the rate of calcite dissolution; for $1 < \Omega < 2.5$, calcite precipitation/dissolution rate was set to zero; and for $\Omega > 2.5$, equations (3–5) were used to calculate calcite precipitation rates. Crystal growth was several orders of magnitude smaller than heterogeneous nucleation for the high DOC concentrations considered (see below), meaning: 1) $R_T \approx R_{HN}$ and thus $R_T \approx 0$ for $\Omega < 2.5$; and 2) calcite precipitation rates were not sensitive to calcite surface area (Lebron and Suarez, 1998).

Standard input values for simulations.—The most important variables influencing calcite precipitation rates include the diffusion coefficient of CO_2 in the outer cortex of the rootlets ($D_{CO2\text{-}outercortex}$), inflow velocity of water (V_{water}), the concentration of DOC in the peat pore water (*DOC*), the surface area of particles that facilitate heterogeneous nucleation of calcite (*SA*), and the respiration rate (R). We chose reasonable and where poorly known generally conservative standard values for use in the modeling (table 1). The standard value for $D_{CO2\text{-}outercortex}$ is half the magnitude of D_{CO2} in pure water, the value for V_{water} is reasonable for peatlands (Gafni and Brooks, 1990), the value for *DOC* is at the high end of the range of values observed in modern tropical peat swamp pore waters (3–6 mM; for example, Gandois and others, 2013; Moore and others, 2013; Müller and others, 2015), the value for *SA* conservatively assumes that calcite nucleation is not catalyzed by surfaces, and the value for R results in P_{CO2} in the peat (below 2 cm) of 0.59 atmospheres.

Post-processing of simulation results.—The COMSOL simulations provide calcite precipitation rates per unit volume of water (fig. 4). To convert these rates into values relevant to our question, we consider the percentage of the peat pore space that would be filled with calcite before being buried below the root zone. To do this, we first calculate the total mass of calcite per unit volume pore space that could have accumulated in the root zone. This value is determined by integrating the steady state calcite precipitation rates over the duration of time in the root zone. The duration depends on peat accumulation rates and the height of the root zone in which calcite precipitates. Because calcite in our model only precipitates around rootlets that extend into the overlying water column and because close spacing of rootlets increases the calcite precipitation rates, we focus on the zone highlighted in figure 4, which is approximately 12 cm tall and is a reasonable approximation of high rootlet density (Hetherington and others, 2016) that may have facilitated coal ball formation. Tropical late Carboniferous peat accumulations rates are constrained by the formation of coal seams <4.3 m thick over tens of thousands of years (Falcon-Lang, 2004). We assume a peat:coal thickness ratio of 10:1, which may overestimate compaction at coalification depths (Nadon, 1998) and almost certainly overestimates compaction of coal ball-bearing coals, the permineralized zones of which preserve undeformed plant fossils suggesting that no compaction occurred. The duration of at least 10,000 years to accumulate 40 m of peat implies a peat accumulation rate of < 4 mm/yr. This rate is broadly consistent with the mean Holocene coastal Indonesian peat accumulation rate of 1.8 mm/yr (Dommain and others, 2011); as such, we use 2 mm/yr in our calculations. At this accumulation rate, a given volume of peat would accumulate calcite for 60 years in the zone of interest. Therefore, we integrate the simulated average steady state calcite precipitation rates in the zone of interest over 60 years to determine the mass of calcite per unit volume of pore space that could have accumulated in the root zone. Using the density of calcite, we then calculate the percentage of the pore spaces filled with calcite.

Peat cementation.—For the standard values, we calculate for the zone of interest that greater than 20 percent of the pore spaces in the peat would be filled with calcite within 60 years. How much cementation is enough cementation? Observed relationships between P-wave velocities and porosity reduction in sandstones provide some insight. The substantial increase in P-wave velocity of sandstones that occur with small decreases (a few %) in porosity near the onset of diagenesis has been interpreted to result from the accumulation of a small volume of cement at grain contacts that substantially stiffens the material (the contact-cement model, for example, Avseth and others, 2010). Diagenetic trends after this initial stiffening have smaller slopes (in porosity-velocity space), but velocities of 3 km/s at >30 percent porosity indicate that lithification can occur due to cement-infilling and/or compaction of less than ¼ of an initial 40 percent porosity (Avseth and others, 2010). Although sandstones are not necessarily a good analogy for peat, it is apparent that preliminary lithification can occur with minimal infilling by cement (2–25% of the initial porosity). Therefore, our modeling with the standard input values is consistent with cementation in the root zone that is sufficient to prevent or limit compaction. Furthermore, the location of cement accumulation (for example at grain contacts or surrounding individual grains) is an important factor for lithification. Our modeling suggests calcite precipitation was concentrated adjacent to living rootlets (up to 70% porosity filled with calcite) and therefore lithified rootlets may have acted as pillars protecting themselves and the intercalated peat (which may have been relatively poorly lithified) from compaction during burial. If our model is correct, then coal balls were formed in the rhizosphere of arborescent lycopsids, explaining their restriction to the Permo-Carboniferous, and were perhaps further mineralized during burial diagenesis, as suggested by petrographic evidence for multiple generations of carbonate mineral precipitation (Raymond and others, 2012; Siewers and Phillips, 2015).

Sensitivity analysis.—We investigated the sensitivity of calculated percent pore filling to several input variables. The water velocity is an important control. A sufficiently high velocity should result in no calcite precipitation because CO_2 does not have time to escape by diffusion. Stagnant water should also result in no calcite precipitation because without an influx of Ca^{2+}, the steady state of the system will be chemical equilibrium at which there is no accumulation of calcite. Therefore, maximum calcite precipitation rates are expected to occur at intermediate water inflow velocities. The simulations indicate that the optimal flow velocity is about 5 mm/day (fig. 5). Velocities above 1.5 cm/day result in calcite precipitation rates that are very small (fig. 5). Sensitivity is lower at low velocities; infilling remains above 5 percent down to 0.2 mm/day (fig. 5).

Sensitivity to DOC is rather small at the elevated DOC levels likely occurring in the peat pore waters. DOC concentrations of 10 mmol/L (double the standard value) result in 18 percent infilling whereas DOC concentrations of 1 mmol/L (20% of the standard value) result in 30 percent infilling. Large increases in calcite precipitation rates occur at lower DOC (below 0.5 mmol/L), but based on modern tropical peat pore waters (Gandois and others, 2013; Moore and others, 2013; Müller and others, 2015) such low DOC is unlikely. Sensitivity to P_{CO2} is also relatively small. The interference of DOC with calcite precipitation decreases with increasing CO_2. The maximum possible pore water P_{CO2} is equal to atmospheric pressure (1.15 atm for the Carboniferous due to elevated atmospheric O_2) because bubbles would form with the addition of more CO_2. Therefore, we used a respiration rate (approximately 2× the standard value) that resulted in 1.15 atm P_{CO2} below 2 cm in the peat to help constrain maximum possible calcite precipitation rates. With a DOC concentration of 1 mmol/L and the elevated respiration rate, we calculate that 39 percent of the pore space could have filled with calcite. An unquantified source of uncertainty here is that we extrapolated equation (4) to higher P_{CO2} than the range over which it was experimentally calibrated (up to 10 kPa). The CO_2 diffusion coefficient in the outer cortex is the most uncertain of the model inputs. However, assuming $D_{CO2\text{-}outercortex}$ values 1 order of magnitude smaller than the value in pure water, we calculate filling approximately 7 percent of the porosity with calcite in 60 years. Thus, if D_{CO2} in the outer cortex was within an order of magnitude of its value in pure water, coal ball formation could have occurred rapidly and shallowly enough to

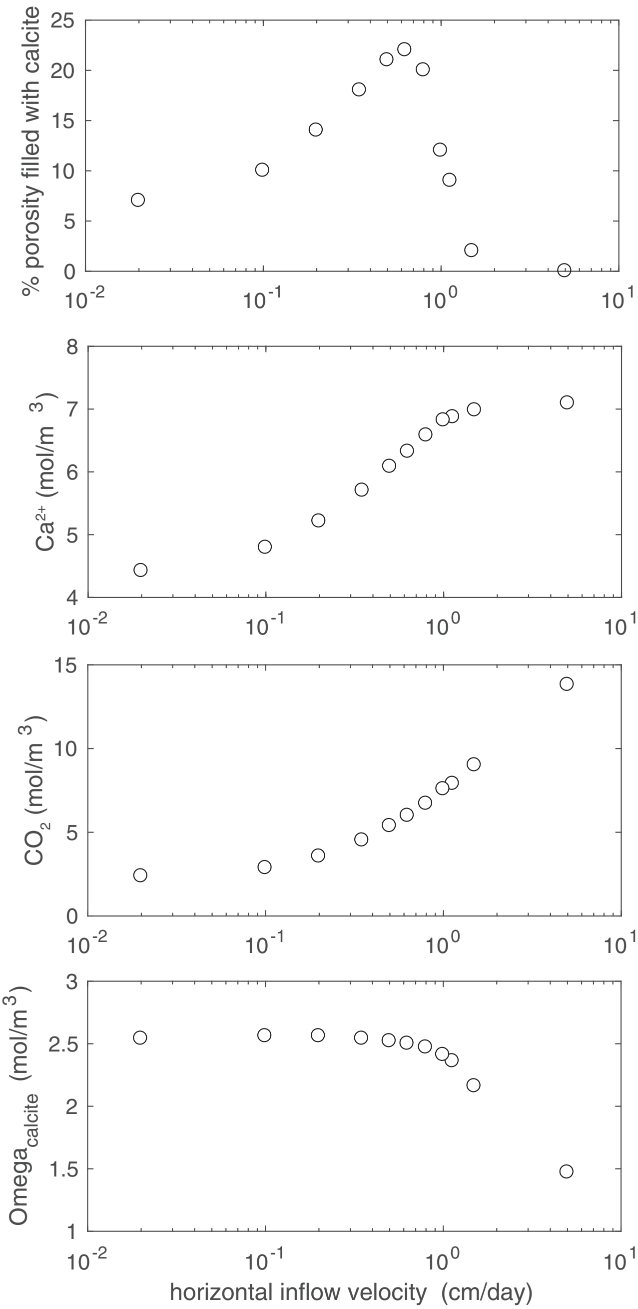

Fig. 5. Sensitivity to water velocity. Calcite precipitation rates are highest at velocities around 5 mm/day. Given these precipitation rates, greater than 20% of the pore spaces within the region highlighted in yellow in figure 4 could have been filled with calcite.

prevent substantial compaction, explaining the exceptional preservation of plant remains. If the outer cortex was a more substantial barrier to diffusion, then our model might only explain coal ball formation under otherwise optimized conditions.

Additional considerations.—Factors we did not consider that would make our model more quantitative include: changes in water flow velocity as calcite fills porosity and thus restricts flow in the peat; the potential that rootlets became cased in calcite thus slowing the escape of CO_2 from pore waters; the growth of roots; and the dynamics of peat compaction during early-stage burial.

The occurrence of arborescent lycopsid-bearing coals without coal balls is perhaps explained by either an insufficiently large calcium flux into those swamps (either due to lack of a sufficiently large Ca^{2+} source or to slow groundwater flow), or to fast groundwater flow limiting the escape of CO_2 from peat within lycopsid stands. The rather rare occurrence of coal balls in coals lacking arborescent lycopsids may be explained by other coal swamp plants with aerenchymatous roots such as the tree fern *Psaronius* (Taylor and others, 2009), which dominated the biomass of coal swamps after the decline of lycopsids during the late Westphalian and early Stephanian across Euramerica (Cleal and others, 2011) before going extinct in the Permian. This raises the more general question about whether roots in other species that are efficient in gas exchange, for example the pneumatophore structures in mangroves, could also facilitate coal ball formation. This warrants further study, but we note that: 1) lycopsids evolved roots independently from all other plants (Hetherington and Dolan, 2017) and so their function may partly differ too; and 2) their root and stem anatomy is unique, particularly with regards to the proportion of space allocated to interconnected air spaces.

SOIL DIVERSITY

The fossil soil record has been interpreted to reflect a monotonic increase in global soil diversity through geologic time (Retallack, 2001). This soil diversification occurred in concert with the evolution of animals and plants. For instance, the evolution of trees with large roots resulted in the appearance of well-drained, moderately leached forest soils called Alfisols (Retallack, 1997), and the coevolution of grasses and grazers resulted in the appearance of soils now closely associated with grasslands called Mollisols (Retallack, 2013). Given the close relationships between plants, animals and soils, and the well-documented extinctions of plants and animals, one might expect that soils should have suffered the same. However, with the exception of green clays that characterized early Precambrian landscapes before the oxygenation of Earth's atmosphere, no loss in soil diversity has been recognized (Retallack, 2001). This leads us to question whether soil diversity and biological diversity are related on geologic timescales. Are soils somehow immune to loss of diversity, or have losses of soil diversity escaped recognition?

If coal balls were pedogenic in origin, then the coals that contain them are best identified as pedogenically permineralized Histosols that were unique to the Permo-Carboniferous. Their properties would have also been unique. They would have been organic carbon rich yet highly indurated, characterized by a thick calcic horizon with low porosity and permeability that may have been overlain by a thin horizon of organic soil material. The occurrence of these soils at many locations in the paleotropics along with their unique properties, their close association with lycopsid (and possibly other aerenchymatous plant) forests, and their unique genesis support the notion that their disappearance from the rock record at the end of the Permian constitutes a substantial loss in soil diversity.

Paleozoic plants were more diverse at the highest taxonomic levels than plants are today (Behrensmeyer and others, 1992). Plant extinctions at the end of the Carboniferous in Euramerica involve pteridosperms (seed ferns) as well as the arborescent lycopsids, and thus represent an important step in the permanent loss of botanical diversity on Earth (Phillips and others, 1985; Behrensmeyer and others, 1992). The evidence presented here for a loss in soil diversity that coincided with a prominent botanical extinction suggests that pedodiversity and botanical diversity were closely related through geologic time, especially when considered alongside the existing evidence for the appearance of new soils with the diversification of plants (Retallack, 1997, 2013). The contemporaneous loss of pedodiversity and botanical diversity raises questions concerning causality and feedbacks. For instance, did the loss of pedogenically permineralized Histosols exacerbate organismal extinctions or was it simply a manifestation of them? Such questions are important, especially in light of modern global change, which has been detrimental to soils globally (Amundson and others, 2015). Indeed, some rare and/or endemic soils are currently considered endangered or locally "extinct" due to historical changes in land use (Amundson and others, 2003; Shangguan and others, 2014). The rock record may help us gauge the implications of this modern change and should help guide the fledgling science of soil conservation.

AUTHOR'S CONTRIBUTIONS

DOB carried out the geochemical modeling and wrote the paper; DLR conceived of the study and compiled the paleobotanical and coal ball occurrence data. Both authors designed the study and approved the final version of the manuscript.

ACKNOWLEDGMENTS

We thank Bob Berner and Leo Hickey (in memoriam), who introduced this topic to DLR, Bayani Cardenas for assistance with COMSOL and Bill DiMichele, Zachary Sharp, Les McFadden, Chris Bell, Lee Nordt and Kyle Spikes for discussion. Thanks to Hermann Pfefferkorn and Nathan Sheldon for helpful reviews.

REFERENCES

Amundson, R., Guo, Y., and Gong, P., 2003, Soil diversity and land use in the United States: Ecosystems, v. 6, n. 5, p. 470–482, https://doi.org/10.1007/s10021-002-0160-2

Amundson, R., Berhe, A. A., Hopmans, J. W., Olson, C., Sztein, A. E., and Sparks, D. L., 2015, Soil and human security in the 21st century: Science, v. 348, n. 6235,p. 1261071, https://doi.org/10.1126/science.1261071

Anderson, T. F., Brownlee, M. E., and Phillips, T. L., 1980, A stable isotope study on the origin of the permineralized peat zones in the Herrin Coal: The Journal of Geology, v. 88, n. 6, p. 713–722, https://doi.org/10.1086/628557

Avseth, P., Mukerji, T., and Mavko, G., 2010, Quantitative seismic interpretation: Applying rock physics tools to reduce interpretation risk: Cambridge, United Kingdom, Cambridge University Press, 376 p.

Baker, R. A., and DiMichele, W. A., 1997, Biomass allocation in Late Pennsylvanian coal-swamp plants: Palaios, v. 12, n. 2, p. 127–132, https://doi.org/10.2307/3515302

Behrensmeyer, A. K., Damuth, J. D., DiMichele, W. A., Potts, R., Sues, H.-D., and Wing, S. L., 1992, Terrestrial Ecosystems Through Time: Chicago, Illinois, The University of Chicago Press, p. 568.

Berner, R. A., 2006a, Geological nitrogen cycle and atmospheric N_2 over Phanerozoic time: Geology, v. 34, n. 5, p. 413–415, https://doi.org/10.1130/G22470.1

_______ 2006b, Inclusion of the weathering of volcanic rocks in the GEOCARBSULF model: American Journal of Science, v. 306, n. 5, p. 295–302, https://doi.org/10.2475/05.2006.01

________ 2009, Phanerozoic atmospheric oxygen: New results using the GEOCARBSULF model: American Journal of Science, v. 309, n. 7, p. 603–606, https://doi.org/10.2475/07.2009.03

Boyce, C. K., and DiMichele, W. A., 2016, Arborescent lycopsid productivity and lifespan: Constraining the possibilities: Review of Palaeobotany and Palynology, v. 227, p. 97–110, https://doi.org/10.1016/j.revpalbo.2015.10.007

Bridgham, S. D., and Richardson, C. J., 1992, Mechanisms controlling soil respiration (CO_2 and CH_4) in southern peatlands: Soil Biology and Biochemistry, v. 24, n. 11, p. 1089–1099, https://doi.org/10.1016/0038-0717(92)90058-6

Buhmann, D., and Dreybrodt, W., 1985, The kinetics of calcite dissolution and precipitation in geologically relevant situations of karst areas: 1. Open system: Chemical Geology, v. 48, N. 1–4, p. 189–211, https://doi.org/10.1016/0009-2541(85)90046-4

Came, R. E., Eiler, J. M., Veizer, J., Azmy, K., Brand, U., and Weidman, C. R., 2007, Coupling of surface temperature and atmospheric CO_2 concentrations during the Palaeozoic era: Nature, v. 449, p. 198–201, https://doi.org/10.1038/nature06085

Chen, B., Joachimski, M. M., Shen, S.-Z., Lambert, L. L., Lai, X.-L., Wang, X.-D., Chen, J., and Yuan, D.-X., 2013, Permian ice volume and palaeoclimate history: Oxygen isotope proxies revisited: Gondwana Research, v. 24, n. 1, p. 77–89, https://doi.org/10.1016/j.gr.2012.07.007

Chimner, R. A., 2004, Soil respiration rates of tropical peatlands in Micronesia and Hawaii: Wetlands, v. 24, p. 51–56, https://doi.org/10.1672/0277-5212(2004)024[0051:SRROTP]2.0.CO;2

Cleal, C. J., Opluštil, S., Thomas, B. A., and Tenchov, Y., 2011, Pennsylvanian vegetation and climate in tropical Variscan Euramerica: Episodes, v. 34, n. 1, p. 3–12.
Curtis, C. D., Coleman, M. L., and Love, L. G., 1986, Pore water evolution during sediment burial from isotopic and mineral chemistry of calcite, dolomite, and siderite concretions: Geochimica et Cosmochimica Acta, v. 50, n. 10, p. 2321–2334, https://doi.org/10.1016/0016-7037(86)90085-2
Cussler, E.L., 2009, Diffusion: Mass transfer in fluid systems: Cambridge University Press, 647 p., https://doi.org/10.1017/CBO9780511805134
de Kanel, J., and Morse, J. W., 1979, A simple technique for surface area determination: Journal of Physics E: Scientific Instruments, v. 12, n. 4, p. 272, https://doi.org/10.1088/0022-3735/12/4/011
DeMaris, P. J., 2000, Formation and distribution of coal balls in the Herrin Coal (Pennsylvanian), Franklin County, Illinois Basin, USA: Journal of the Geological Society, London, v. 157, n. 1, p. 221–228, https://doi.org/10.1144/jgs.157.1.221
DeMaris, P. J., Bauer, R. A., Cahill, R. A., and Damberger, H. H., 1983, Geologic Investigation of roof and floor strata: Longwall demonstration, Old Ben Mine No. 24: Prediction of coal balls in the Herrin Coal Illinois: State Geological Survey Final Technical Report, Volume 2, p. 1–69, https://doi.org/10.5962/bhl.title.62150
DiMichele, W. A., and DeMaris, P. J., 1987, Structure and dynamics of a Pennsylvanian-age Lepidodendron forest: Colonizers of a disturbed swamp habitat in the Herrin (No. 6) coal of Illinois: Palaios, v. 2, n. 2, p. 146–157, https://doi.org/10.2307/3514642
DiMichele, W. A., and Phillips, T. L., 1985, Arborescent lycopod reproduction and paleoecology in a coal-swamp environment of late Middle Pennsylvanian age (Herrin Coal, Illinois, USA): Review of Palaeobotany and Palynology, v. 44, n. 1–2, p. 1–26, https://doi.org/10.1016/0034-6667(85)90026-0
_______ 1994, Paleobotanical and paleoecological constraints on models of peat formation in the Late Carboniferous of Euramerica: Palaeogeography, Palaeoclimatology, Palaeoecology, v. 106, n. 1–4, p. 39–90, https://doi.org/10.1016/0031-0182(94)90004-3
Dommain, R., Couwenberg, J., and Joosten, H., 2011, Development and carbon sequestration of tropical peat domes in south-east Asia: Links to post-glacial sea-level changes and Holocene climate variability: Quaternary Science Reviews, v. 30, n. 7–8, p. 999–1010, https://doi.org/10.1016/j.quascirev.2011.01.018
Dreybrodt, W., 1980, Deposition of calcite from thin films of natural calcareous solutions and the growth of speleothems: Chemical Geology, v. 29, n. 1–4, p. 89–105, https://doi.org/10.1016/0009-2541(80)90007-8
_______ 1981, Mixing corrosion in $CaCO_3/1bCO_2/1bH_2O$ systems and its role in the karstification of limestone areas: Chemical Geology, v. 32, n. 1–4, p. 221–236, https://doi.org/10.1016/0009-2541(81)90145-5
Dreybrodt, W., Eisenlohr, L., Madry, B., and Ringer, S., 1997, Precipitation kinetics of calcite in the system $CaCO_3$-H_2O-CO_2: The conversion to CO_2 by the slow process $H^+ + HCO_3^- \rightarrow CO_2 + H_2O$ as a rate limiting step: Geochimica et Cosmochimica Acta, v. 61, n. 18, p. 3897–3904, https://doi.org/10.1016/S0016-7037(97)00201-9
Evans, W. D., and Amos, D. H., 1961, An example of the origin of coal balls: Proceedings of the Geologists' Association, v. 72, n. 4, p. 445–454, https://doi.org/10.1016/S0016-7878(61)80038-2
Falcon-Lang, H. J., 2004, Pennsylvanian tropical rain forests responded to glacial-interglacial rhythms: Geology, v. 32, n. 8, p. 689–692, https://doi.org/10.1130/G20523.1
Farkas, J., Böhm, F., Wallmann, K., Blenkinsop, J., Eisenhauer, A., van Geldern, R., Munnecke, A., Voigt, S., and Veizer, J., 2007, Calcium isotope record of Phanerozoic oceans: Implications for chemical evolution of seawater and its causative mechanisms: Geochimica et Cosmochimica Acta, v. 71, n. 21, p. 5117–5134, https://doi.org/10.1016/j.gca.2007.09.004
Gafni, A., and Brooks, K. N., 1990, Hydraulic characteristics of four peatlands in Minnesota: Canadian Journal of Soil Science, v. 70, n. 2, p. 239–253, https://doi.org/10.4141/cjss90-025
Gandois, L., Cobb, A. R., Hei, I. C., Lim, L. B., Salim, K. A., and Harvey, C. F., 2013, Impact of deforestation on solid and dissolved organic matter characteristics of tropical peat forests: Implications for carbon release: Biogeochemistry, v. 114, n. 1–3, p. 183–199, https://doi.org/10.1007/s10533-012-9799-8
Gifford, E. M., and Foster, A. S., 1989, Morphology and evolution of vascular plants, 3rd edition: New York, New York, W. H. Freeman, 626 p.
Gradstein, F. M., Ogg, J. G., Schmitz, M. D., and Ogg, G. M., 2012, The Geologic Time Scale 2012: Amsterdam, Elsevier, p. 1144.
Green, W. A., 2010, The function of the aerenchyma in arborescent lycopsids: Evidence of an unfamiliar metabolic strategy: Proceedings of the Royal Society B, v. 277, p. 2257–2267, https://doi.org/10.1098/rspb.2010.0224
_______ 2014, The parichos problem and the function of aerenchyma in the Lycopsida: Bulletin of the Peabody Museum of Natural History, v. 55, n. 2, p. 191–200, https://doi.org/10.3374/014.055.0206
Hetherington, A. J., and Dolan, L., 2017, The evolution of lycopsid rooting structures: Conservatism and disparity: New Phytologist, v. 215, n. 2, p. 538–544, https://doi.org/10.1111/nph.14324
Hetherington, A. J., Berry, C. M., and Dolan, L., 2016, Networks of highly branched stigmarian rootlets developed on the first giant trees: Proceedings of the National Academy of Sciences of the United States of America, v. 113, n. 24, p. 6695–6700, https://doi.org/10.1073/pnas.1514427113
Hilton, J., Rothwell, G. W., Li, C., Wang, S., and Galtier, J., 2001, Permineralized cardiocarpalean ovules in wetland vegetation from Early Permian volcaniclastic sediments of China: Palaeontology, v. 44, n. 5, p. 811–825, https://doi.org/10.1111/1475-4983.00202
Hooker, J. D., and Binney, W. W., 1855, On the structure of certain limestone nodules enclosed in seams of bituminous coal, with a description of some triginocarpons contained in them: Philosophical Transactions of the Royal Society B, v. 145, p. 149–156, https://doi.org/10.1098/rstl.1855.0006
Isbell, J. L., Henry, L. C., Gulbranson, E. L., Limarino, C. O., Fraiser, M. L., Koch, Z. J., Ciccioli, P. L., and Dineen, A. A., 2012, Glacial paradoxes during the late Paleozoic ice age: Evaluating the equilibrium line

altitude as a control on glaciation: Gondwana Research, v. 22, n. 1, p. 1–19, https://doi.org/10.1016/j.gr.2011.11.005
Lebron, I., and Suarez, D. L., 1998, Kinetics and mechanisms of precipitation of calcite as affected by P_{CO2} and organic ligands at 25 °C: Geochimica et Cosmochimica Acta, v. 62, n. 3, p. 405–416, https://doi.org/10.1016/S0016-7037(97)00364-5
Li, X., and Yao, Z., 1982, A review of recent research on the Cathaysia flora in Asia: American Journal of Botany, v. 69, p. 479–486, https://doi.org/10.1002/j.1537-2197.1982.tb13282.x
Li, X., Shen, G., Tian, B., Wang, S., and Ouyang, S., 1995, Some notes on Carboniferous and Permian floras in China, *in* Li, X., editor, Fossil Floras of China through the Geological Ages: Guangzhou, Guangdong Science and Technology Press, p. 244–302.
Love, L. G., Coleman, M. L., and Curtis, C. D., 1983, Diagenetic pyrite formation and sulphur isotope fractionation associated with a Westphalian marine incursion, northern England: Transactions of the Royal Society of Edinburgh: Earth Sciences, v. 74, n. 3, p. 165–182, https://doi.org/10.1017/S0263593300009822
Mamay, S. H., and Yochelson, E. L., 1962, Occurrence and significance of marine animal remians in American coal balls: United States Geological Survey Professional Paper, v. 354-I, p. 193–224, https://doi.org/10.3133/pp354I
Massman, W. J., 1998, A review of the molecular diffusivities of H_2O, CO_2, CH_4, CO, O_3, SO_2, NH_3, N_2O, NO and NO_2 in air, O_2 and N_2 near STP: Atmospheric Environment, v. 32, n. 6, p. 1111–1127, https://doi.org/10.1016/S1352-2310(97)00391-9
Moore, S., Evans, C. D., Page, S. E., Garnett, M. H., Jones, T. G., Freeman, C., Hooijer, A., Wiltshire, A. J., Limin, S. H., and Gauci, V., 2013, Deep instability of deforested tropical peatlands revealed by fluvial organic carbon fluxes: Nature, v. 493, p. 660, https://doi.org/10.1038/nature11818
Müller, D., Warneke, T., Rixen, T., Müller, M., Jamahari, S., Denis, N., Mujahid, A., and Notholt, J., 2015, Lateral carbon fluxes and CO_2 outgassing from a tropical peat-draining river: Biogeosciences, v. 12, p. 5967–5979, https://doi.org/10.5194/bg-12-5967-2015
Nadon, G. C., 1998, Magnitude and timing of peat-to-coal compaction: Geology, v. 26, n. 8, p. 727–730, https://doi.org/10.1130/0091-7613(1998)026<0727:MATOPT>2.3.CO;2
Niklas, K. J., Tiffney, B. H., and Knoll, A. H., 1985, Patterns in vascular land plant diversification: An analysis at the species level, *in* Valentine, J., editor, Phanerozoic Diversity Patterns: Profiles in Macroevolution: Princeton, New Jersey, Princeton University Press, Princeton Series in Geology and Paleontology, n. 44, p. 97–127, https://doi.org/10.1515/9781400855056.97
Perkins, T. W., 1976, Textures and conditions of formation of Middle Pennsylvanian coal balls, central united States: University of Kansas, Paleontological Contributions, v. 82, p. 1–13.
Phillips, S., and Bustin, R. M., 1996, Sulfur in the Changuinola peat deposit, Panama, as an indicator of the environments of deposition of peat and coal: Journal of Sedimentary Research, v. 66, n. 1, p. 184–196, https://doi.org/10.1306/D42682F2-2B26-11D7-8648000102C1865D
Phillips, T. L., 1980, Stratigraphic and geographic occurrrences of perminieralized coal-swamp plants–Upper Carboniferous of North America and Europe, *in* Dilcher, D. L., and Taylor, T. N., editors, Biostratigraphy of Fossil Plants: Stroudsburg, Pennsylvania, Dowden, Hutchinson and Ross, p. 25–92.
_______ 1981, Stratigraphic occurrences and vegetational patterns of Pennsylvanian pteridosperms in Euramerican coal swamps: Review of Palaeobotany and Palynology, v. 32, n. 1, p. 5–26, https://doi.org/10.1016/0034-6667(81)90073-7
Phillips, T. L., and DiMichele, W. A., 1992, Comparative ecology and life-history biology of arborsecent lycopsids in the late Carboniferous swamps of Euramerica: Annals of the Missouri Botanical Garden, v. 79, n. 3, p. 560–588, https://doi.org/10.2307/2399753
Phillips, T. L., and Peppers, R. A., 1984, Changing patterns of Pennsylvanian coal-swamp vegetation and implications of climatic control on coal occurrence: International Journal of Coal Geology, v. 3, n. 3, p. 205–255, https://doi.org/10.1016/0166-5162(84)90019-3
Phillips, T. L., Peppers, R. A., and DiMichele, W. A., 1985, Stratigraphic and interregional changes in Pennsylvanian coal-swamp vegetation: Environmental inferences: International Journal of Coal Geology, v. 5, n. 1–2, p. 43–109, https://doi.org/10.1016/0166-5162(85)90010-2
Plummer, L. N., Wigley, T. M. L., and Parkhurst, D. L., 1978, The kinetics of calcite dissolution in CO_2-water systems at 5° to 60°C and 0.0 to 1.0 atm CO_2: American Journal of Science, v. 278, n. 2, p. 179–216, https://doi.org/10.2475/ajs.278.2.179
Rao, C. P., 1984, Origin of coal balls in the Illinois Basin, 9th International Congress on Carboniferous Stratigraphy and Geology (IX-ICC): Carnbondale, Illinois, Southern Illinois University Press, p. 393–406.
Raymond, A., Lambert, L., Costanza, S., Slone, E. J., and Cutlip, P. C., 2010, Cordaiteans in paleotropical wetlands: An ecological re-evaluation: International Journal of Coal Geology, v. 83, n. 2–3, p. 248–265, https://doi.org/10.1016/j.coal.2009.10.009
Raymond, A., Guillemette, R., Jones, C. P., and Ahr, W. M., 2012, Carbonate petrology and geochemistry of Pennsylvanian coal balls from the Kalo Formation of Iowa: International Journal of Coal Geology, v. 94, p. 137–149, https://doi.org/10.1016/j.coal.2012.01.007
Retallack, G. J., 1997, Early forest soils and their role in Devonian global change: Science, v. 276, n. 5312, p. 583–585, https://doi.org/10.1126/science.276.5312.583
_______ 2001, Soils of the Past: An Introduction to Paleopedology: Oxford, England, Blackwell Science Ltd, 404 p.
______ 2013, Global cooling by grassland soil of the geological past and near future: Annual Review of Earth and Planetary Sciences, v. 41, p. 69–86, https://doi.org/10.1146/annurev-earth-050212-124001
Reynolds, O., 1883, An experimental investigation of the circumstances which determine whether the motion of water shall be direct or sinuous, and of the law of resistance in parallel channels:

Philosophical Transactions of the Royal Society of London, v. 174, p. 935–982, https://doi.org/10.1098/rstl.1883.0029

Royer, D. L., 2014, Atmospheric CO_2 and O_2 during the Phanerozoic: Tools, patterns, and impacts, *in* Holland, H. D., and Turekian, K.K., editors, Treatise on Geochemistry (Second Edition), volume 6: Oxford, Elsevier, p. 251–267, https://doi.org/10.1016/B978-0-08-095975-7.01311-5

Royer, D. L., Donnadieu, Y., Park, J., Kowalczyk, J., and Goddéris, Y., 2014, Error analysis of CO_2 and O_2 estimates from the long-term geochemical model GEOCARBSULF: American Journal of Science, v. 314, n. 9, p. 1259–1283, https://doi.org/10.2475/09.2014.01

Schopf, J. M., 1975, Modes of fossil preservation: Review of Palaeobotany and Palynology, v. 20, n. 1–2, p. 27–53, https://doi.org/10.1016/0034-6667(75)90005-6

Scott, A. C., and Rex, G. M., 1985, The formation and significance of Carboniferous coal balls: Philosophical Transactions of the Royal Society B, v. 311, p. 123–137, https://doi.org/10.1098/rstb.1985.0144

Scott, A. C., Mattey, D. P., and Howard, R., 1996, New data on the formation of Carboniferous coal balls: Review of Palaeobotany and Palynology, v. 93, n. 1–4, p. 317–331, https://doi.org/10.1016/0034-6667(95)00132-8

Shangguan, W., Gong, P., Liang, L., Dai, Y., and Zhang, K., 2014, Soil Diversity as affected by land use in China: Consequences for soil protection: The Scientific World Journal, v. 2014, 12 p., https://doi.org/10.1155/2014/913852

Siewers, F. D., and Phillips, T. L., 2015, Petrography and microanalysis of Pennsylvanian coal-ball concretions (Herrin Coal, Illinois Basin, USA): Bearing on fossil plant preservation and coal-ball origins: Sedimentary Geology, v. 329, p. 130–148, https://doi.org/10.1016/j.sedgeo.2015.07.004

Spencer, A. R. T., Wang, S.-J., Dunn, M. T., and Hilton, J., 2013, Species of the medullosan ovule *Stephanospermum* from the Lopingian (late Permian) floras of China: Journal of Asian Earth Sciences, v. 76, p. 59–69, https://doi.org/10.1016/j.jseaes.2013.07.030

Spicer, R. A., 1989, The formation and interpretation of plant fossil assemblages: Advances in Botanical Research, v. 16, p. 95–191, https://doi.org/10.1016/S0065-2296(08)60240-2

Stewart, W. N., 1947, A comparative study of stigmarian appendages and *Isoetes* roots: American Journal of Botany, v. 34, n. 6, p. 315–324, https://doi.org/10.1002/j.1537-2197.1947.tb12995.x

Stopes, M. C., and Watson, D. M. S., 1909, On the present distribution and origin of the calcareous concretions in coal seams, known as 'coal balls': Philosophical Transactions of the Royal Society of London B, v. 200, p. 167–218, https://doi.org/10.1098/rstb.1909.0005

Sundari, S., Hirano, T., Yamada, H., Kusin, K., and Limin, S., 2012, Effect of groundwater level on soil respiration in tropical peat swamp forests: Journal of Agricultural Meteorology, v. 68, n. 2, p. 121–134, https://doi.org/10.2480/agrmet.68.2.6

Taylor, T. N., Taylor, E. L., and Krings, M., 2009, Paleobotany: The Biology and Evolution of Fossil Plants: Amsterdam, Netherlands, Academic Press, 1252 p.

Tian, B., Wang, S. J., Guo, Y. T., Chen, G., and Zhao, H., 1996, Flora of Palaeozoic coal balls of China: Palaeobotanist, v. 45, p. 247–254.

Tweel, A. W., and Turner, R. E., 2012, Landscape-scale analysis of wetland sediment deposition from four tropical cyclone events: PLOS ONE, v. 7, p. e50528, https://doi.org/10.1371/journal.pone.0050528

Wang, S.-J., Hilton, J., and Tian, B., 2003, A new species of permineralised cardiocarpalean ovule from the Early Permian Taiyuan Formation of northern China: Review of Palaeobotany and Palynology, v. 123, n. 3–4, p. 303–319, https://doi.org/10.1016/S0034-6667(02)00219-1

Wang, Z., 1985, Palaeovegetation and plate tectonics: Palaeophytogeography of North China during Permian and Triassic times: Palaeogeography, Palaeoclimatology, Palaeoecology, v. 49, n. 1–2, p. 25–45, https://doi.org/10.1016/0031-0182(85)90003-3

Weber, J. N., and Keith, M. L., 1962, Carbon-isotope composition and the origin of calcaerous coal balls: Science, v. 138, n. 3543, p. 900–902, https://doi.org/10.1126/science.138.3543.900

Zodrow, E. L., Lyons, P. C., and Millay, M. A., 1996, Geochemistry of autochthonous and hypautochthonous siderite-dolomite coal-balls (Foord Seam, Bolsovian, Upper Carboniferous), Nova Scotia, Canada: International Journal of Coal Geology, v. 29, n. 1–3, p. 199–216, https://doi.org/10.1016/0166-5162(95)00008-9